Heterogeneous nucleation of three-dimensional protein nanocrystals

Georgieva, D.G.; Kuil, M.E.; Oosterkamp, T.H.; Zandbergen, H.W.; Abrahams, J.P.

Acta Crystallographica Section D
Biological Crystallography
ISSN 0907-4449

Heterogeneous nucleation of three-dimensional protein nanocrystals

Dilyana G. Georgieva,[a]* Maxim E. Kuil,[a] Tjerk H. Oosterkamp,[b] Henny W. Zandbergen[c] and Jan Pieter Abrahams[a]

[a]Department of Biophysical and Structural Chemistry, Leiden University, The Netherlands, [b]Leiden Institute of Physics, Leiden University, The Netherlands, and [c]Institute for Metal Reserach and Kavli Institute of Nanoscience, Delft University of Technology, The Netherlands

Correspondence e-mail: d.georgieva@chem.leidenuniv.nl

Received 1 November 2006
Accepted 15 February 2007

Nucleation is the rate-limiting step in protein crystallization. Introducing heterogeneous substrates may in some cases lower the energy barrier for nucleation and thereby facilitate crystal growth. To date, the mechanism of heterogeneous protein nucleation remains poorly understood. In this study, the nucleating properties of fragments of human hair in crystallization experiments have been investigated. The four proteins that were tested, lysozyme, glucose isomerase, a polysaccharide-specific Fab fragment and potato serine protease inhibitor, nucleated preferentially on the hair surface. Macrocrystals and showers of tiny crystals of a few hundred nanometres thickness were obtained also under conditions that did not produce crystals in the absence of the nucleating agent. Cryo-electron diffraction showed that the nanocrystals diffracted to at least 4 Å resolution. The mechanism of heterogeneous nucleation was studied using confocal fluorescent microscopy which demonstrated that the protein is concentrated on the nucleating surface. A substantial accumulation of protein was observed on the sharp edges of the hair's cuticles, explaining the strong nucleating activity of the surface.

1. Introduction

An essential part of most protein crystallographic studies is finding suitable conditions for growing crystals which is often the rate-limiting step.

To predict protein nucleation and crystallization, techniques such as dynamic light scattering (Berne & Pecora, 1976; George & Wilson, 1994) and fluorescence correlation spectroscopy (Schmauder *et al.*, 2002) have been applied. Most studies based on these techniques have shown that the second virial coefficient B_{22} of the dilute protein solution is closely related to protein crystallization (George & Wilson, 1994; Velev *et al.*, 1998; Narayanan & Liu, 2003). Only a narrow range of slightly negative B_{22} values are favourable for crystallization. Working under conditions outside this range reduces the possibility of a successful outcome. However, using conditions which correspond to the so-called 'crystallization window' does not guarantee a successful crystallization trial. Thus, finding a crystallization condition remains a process of trial and error.

Progress in the miniaturization and automation of crystallization experiments led to the development of protein nanocrystallization, which has made it possible to set up thousands of crystallization trials in a single experiment.

Despite the large number of proteins and screening conditions that have been tested, the success rate is lower than expected (Dale *et al.*, 2003). It appears that nanocrystallization is not a simple miniaturization of a protein-crystallization experiment and that one cannot reduce the crystallization volume without paying a penalty. In nanovolumes, surface-tension forces become more prominent and might have effects on the nucleation event. Furthermore, Bodenstaff *et al.* (2002) showed that the mean number of nuclei formed per unit volume is linearly proportional to the volume of the mother liquor. Moreover, when working in a nanolitre regime, the time before the first nuclei are formed increases dramatically. This is on top of already poor crystallization even in larger volumes.

It is known that the protein should be in the metastable phase for crystal growth, but that higher levels of saturation are needed for nucleation. In many crystallization experiments the required saturation levels are not reached, so that nucleation does not occur. To create an environment that favours nucleation, so-called nucleant agents are introduced into the crystallization droplet that create a higher local concentration of macromolecules and thus lower the energy barrier for nucleation. A search for a 'universal nucleant' has been ongoing for two decades. To date, the following lines of research have been pursued.

(i) McPherson introduced the idea of controlling nucleation by using mineral substrates as epitaxic nucleants for protein crystallization (McPherson & Shlichta, 1987). His initiative has been pursued for more than 15 y by employing a variety of substrates, but so far none of them have been generally adopted.

(ii) Subsequently, the idea of using lipid layers and protein monolayers of two-dimensional crystals was introduced, which also improved the crystallization of three-dimensional protein crystals (Hemming *et al.*, 1995). More recently, Fermani *et al.* (2001) demonstrated that substrates containing ionizable surface groups can also enhance the crystallization of certain proteins.

(iii) The idea of using natural seedlings (whiskers, seeds, fibres *etc.*) to generate nucleation in crystallization experiments is another approach that has been successfully applied in protein crystallography (D'Arcy *et al.*, 2003).

(iv) The development of lithography techniques allowed the fabrication of a variety of silicon substrates with different surface characterizations: terraces, steps and even pores of a few nanometres in size that can match a crystal lattice. Sanjoh *et al.* (2001) and Chayen *et al.* (2001) have explored this field intensively and showed that in general structured surfaces appear to be more efficient than nonstructured.

We decided to search for materials which combine as well as possible most of the properties mentioned above: surface ordered at the molecular level, ionizable groups, lipid layers, local concentration cavities, nano- and mesoscopic structure. We found that a prime candidate for such a material was abundantly available: the surface of human hair matches the above criteria quite well. We observed that not only standard proteins such as lysozyme and glucose isomerase but also more difficult proteins such as a polysaccharide-specific Fab fragment and a potato protease inhibitor under study in our laboratory crystallized preferentially on strands of hair.

By using a combination of advanced visualization techniques such as confocal fluorescent microscopy and atomic force microscopy (AFM), it was possible to visualize the distribution of protein on the surface of the hair and demonstrate accumulation of protein on the sharp edges of the hair's cuticles. This experimental observation correlated with numerical simulations published by Cacciuto *et al.* (2004), which showed nucleation and crystallization of a model colloid to occur preferentially on curved surfaces.

2. Experimental procedures

2.1. Materials

The commercial proteins used in this study were chicken egg-white lysozyme (Sigma; EC 3.2.1.17) and glucose isomerase (Hampton Research catalogue No. HR7-100). Antipolymeric Lewis X Fab fragment 54 was expressed by papain digestion of MAP 54-5C10-A followed by extensive purification using affinity and ion-exchange chromatography as described previously by van Roon *et al.* (2004). Potato serine protease inhibitor 6.1 (the number represents the isolectric point) was expressed and purified following the procedure described by Thomassen *et al.* (2004). All chemicals used in the crystallization experiments were purchased from Merck and solutions were further filtered with Millipore filters (0.22 µm) directly before use. Lysozyme was labelled with fluorescein isothiocyanate (Isomer I, Molecular Probes, Eugene, Oregon, USA) for confocal fluorescent studies. Water clear urethane rubber (Clear Flex 50, Smooth-On Inc., Pennsylvania, USA) and polydimethylsiloxane (Sylgard R 184 curing agent silicone elastomer, Dow Corning Corporation, Michigan, USA) were used for preparation of the polymer hair replica. Dark-pigmented human hair fibres were used as heterogeneous nucleant surfaces.

2.2. Crystallization experiments

Crystallization trials were carried out at 293 K using the sitting-drop vapour-diffusion technique in Q crystallization plates (Hampton Research). 1 µl portions of protein solution were added to 1 µl reservoir solution in a sitting drop. For the heterogeneous crystallization of lysozyme, strands of hair were introduced into crystallization droplets containing 7.5 mg ml^{-1} lysozyme, 0.1 *M* acetate buffer pH 4.5, 1.6 *M* NaCl and into conditions containing 7.5 mg ml^{-1} lysozyme, 0.1 *M* acetate buffer pH 4.5, 30% glycerol and a salt concentration varying between 0.65 and 1.6 *M* NaCl.

Glucose isomerase was crystallized in the presence of 2 *M* ammonium sulfate and 0.1 *M* sodium citrate pH 6.5. A final protein concentration of 15 mg ml^{-1} was used for the heterogeneous crystallization. Antipolymeric Lewis X Fab fragment 54 was crystallized in 100 m*M* citrate buffer pH 5 and 11% PEG 3350. Potato serine protease inhibitor was crystallized in 0.1 *M* HEPES pH 7.5, 5% PEG 8000 and 4%

ethylene glycol complemented with 0.1 *M* glycine (Hampton Additive Screen 2). The protein concentration was 7 mg ml^{-1}.

2.3. Chemical modification of the hair surface

Removal of lipids was performed by soaking in petroleum ether. Single hairs were treated with petroleum ether for 30 min (3 × 10 min using fresh portions of the solvent). The remaining petroleum ether was allowed to evaporate and the fibres were washed with the buffer used in the crystallization experiment. A combination of delipification and a slight denaturing of the keratin surface was performed using 50% ethanol solution. The same treatment was performed as described for the petroleum ether. For denaturation of the surface proteins, the hair was subjected to 3 *M* NaOH for 3 min and washed with buffer as in the previous two treatments.

2.4. Preparation of polymer hair replicas

A hair fibre cleaned of dust and impurities using petroleum ether as described in §2.3 was placed on a microscope glass slide and glued at both ends. Polyurethane (Clear Flex 50) was poured onto the fibre, forming a thin layer on the microscope slide. The polyurethane rubber was left overnight at 343 K for complete polymerization. The polymer layer was then detached from the cover slide and the replica of the fibre formed in the polyurethane mould was filled with a second polymer, polydimethylsiloxane, and left for 24 h at 343 K. The polydimethylsiloxane fibre was then removed from the polyurethane rubber mould and further crystallization experiments were performed.

2.5. Atomic force microscopy studies

In situ lysozyme crystallization experiments were set up in a liquid AFM cell. The crystallization composition was the same as described in §2.2. The hair fibre used in this experiment was treated with petroleum ether (§2.3) in order to remove impurities from the fibre that might retract the AFM tip. Petri dishes with water were placed in the AFM to prevent the sample droplet from drying out during imaging. The experiment was performed with a Digital Instruments Nanoscope IIIa scanning-probe. Silicon nitride tips were used throughout in tapping and contact mode with scan frequency varying from 1 to 10 Hz.

2.6. Confocal fluorescence experiments

10 mg ml^{-1} lysozyme dissolved in 10 m*M* carbonate/bicarbonate buffer pH 9.2 was mixed with 1 mg ml^{-1} fluorescein isothiocyanate in dimethylformamide in a ratio of 1:0.65. The mixture was wrapped in aluminium foil and incubated on a rotory shaker at low speed at room temperature. To separate the free dye from the labelled protein, a PD-10 desalting gel-filtration column (Sephadex TM G-25M prepacked column)

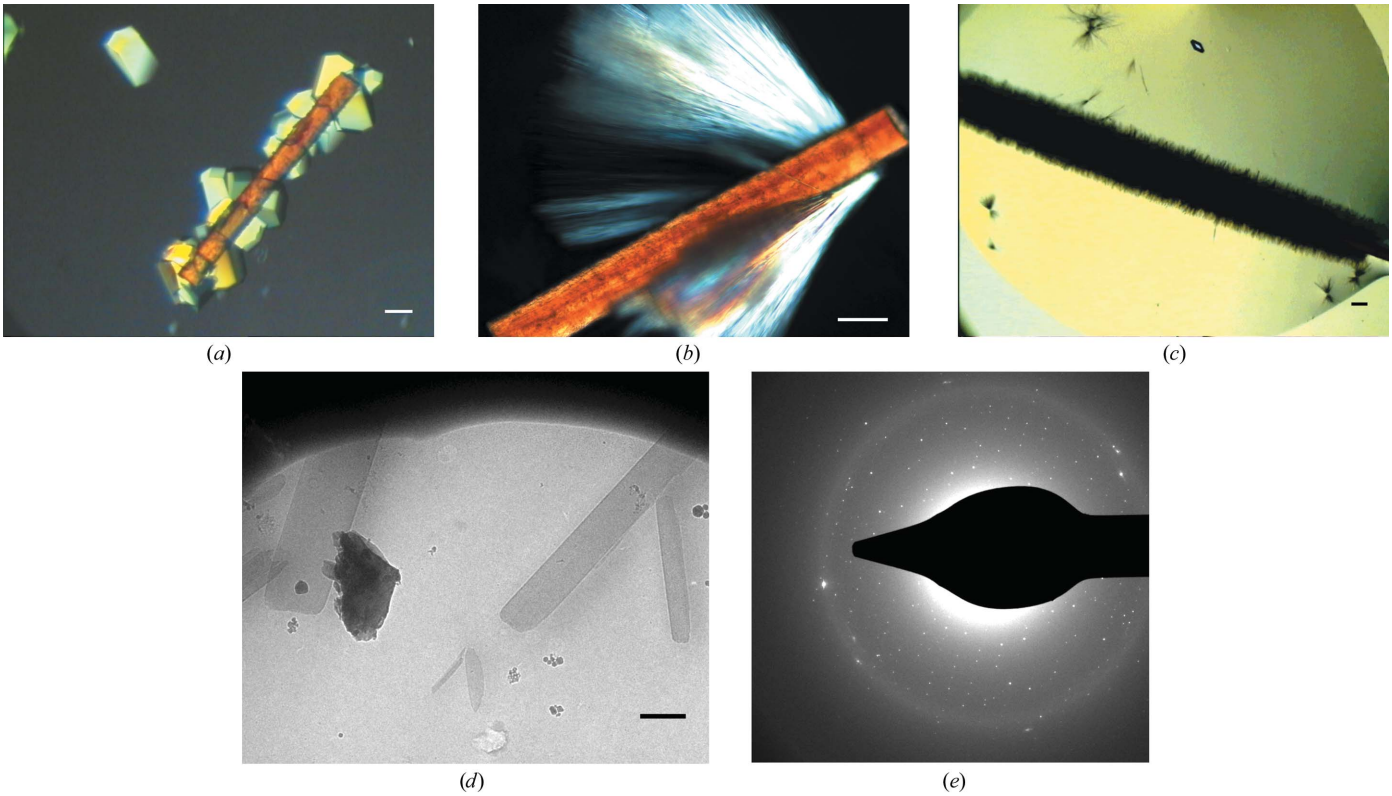

Figure 1
Lysozyme crystals grown heterogeneously on hair fibres in crystallization conditions containing 0.1 *M* sodium acetate pH 4.5, 1.6 *M* sodium chloride and 7.5 mg ml^{-1} protein: (*a*) tetragonal, (*b*) needle-like and (*c*) 'sea-urchin' crystal forms. Scale bars correspond to 100 µm. (*d*) Lysozyme 'sea-urchin' crystals in vitrified ice; scale bar, 1.5 µm. (*e*) Electron diffraction of a frozen 'sea-urchin' lysozyme crystal.

was used. The column was first equilibrated with MilliQ water and then loaded with 825 µl reaction mixture and eluted with MilliQ water. 1 ml fractions were collected. The labelled protein eluted in fractions 4–7. After gel electrophoresis of the collected fractions on a 15% PAGE gel, fluorescent bands were clearly visible in fractions 4–7. After Coomassie staining, these bands corresponded to protein of MW 14.5 kDa, as expected for labelled lysozyme.

Strands of hair were introduced into droplets containing 0.1 *M* acetate buffer pH 4.5, 1.6 *M* NaCl and protein concentrations of 7.5, 2.5, 1 and 0.5 mg ml^{-1} labelled protein and incubated for 4 h at room temperature. The fibres were then removed from the original droplets and placed into new droplets containing the same crystallization agents but without protein. This was performed in order to enhance the visibility of bound fluorescent protein and to reduce the background fluorescence arising from unbound fluorescent protein. Only in this way could the differences in distribution of protein on and near the hair strands be studied using confocal microscopy. For imaging, we used an upright Zeiss Axioplan epifluorescence microscope and a confocal inverted Leica IRBE microscope coupled to an SP1 scanhead with a separate argon and krypton laser. The argon laser was used for excitation at 488 nm and the krypton laser for excitation at 568 nm.

2.7. Sample preparation and electron diffraction of the nano-sized protein crystals

A hair fibre covered with tiny crystals of lysozyme or potato protease inhibitor was placed on a negatively charged 300 mesh continuous carbon grid. Next, a few microlitres of crystallization solution with the same composition as used for crystal growth was pipetted onto the grid, which resulted in the detachment of most of the crystals. After this, the hair fibre was gently removed. The grid with protein crystals was blotted between filter papers and plunge-frozen in liquid ethane using a Vitrobot blotting system. Transmission electron microscopy was performed with a Tecnai F20 FEG microscope in low-dose mode or with a CM30T LaB6 operated at 200 and 300 keV, respectively.

3. Results and discussion

3.1. Examples of heterogeneous nucleation on the surface of human hair

Chicken egg-white lysozyme was used as a model protein for our initial studies. In the presence of hair strands introduced into droplets containing 7.5 mg ml^{-1} lysozyme, 0.1 *M* acetate buffer pH 4.5 and 1.6 *M* NaCl, it was observed that lysozyme has a clear tendency to crystallize on the fibres. Fig. 1 shows three morphological crystal forms of the protein to nucleate preferentially on the selected heterogeneous substrates. The induction time for nucleation was also much shorter: crystals were observed to appear within 4 h on the hair strands, while more than 10 h was needed to form crystals in bulk solution. In some cases coexistence of tetragonal and 'sea-urchin' crystals was observed on the same nucleant surface. Such a coexistence of crystal forms has been observed previously in bulk solution (Lorber *et al.*, 1996; Bodenstaff *et al.*, 2002). A tetragonal lysozyme crystal grown on hair was mounted in a capillary and X-ray diffraction confirmed space group $P4_32_12$ (data not shown). In our further experiments, we consistently reproduced the crystallization of the macro and nano 'sea-urchin' crystals on the selected nucleant surface. In the presence of hair fibres, crystals were also obtained in conditions under which nucleation does not occur or occurs very rarely. For example, the inclusion of 30% glycerol prevents nucleation of lysozyme in bulk solution at a concentration of 7.5 mg ml^{-1}. However, when hair strands were introduced into such a mother liquor, we observed lysozyme crystals nucleating and growing on the hair in a range of salt concentrations between 0.65 and 1.6 *M* NaCl, confirming the strong nucleating properties of this surface. For the crystallization experiments two different strands of human hair were used; both were dark-pigmented. No major differences in crystallization behaviour were observed. We did not

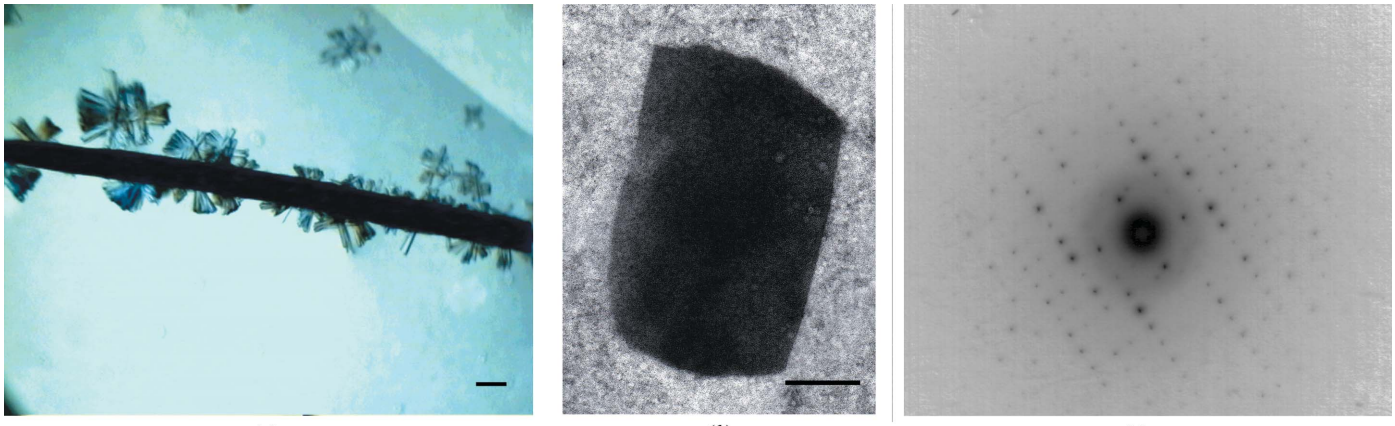

(*a*) (*b*) (*c*)

Figure 2
Examples of protein crystals grown heterogeneously on strands of hair. (*a*) Potato serine protease inhibitor crystals originating from heterogeneous nucleation on a hair fibre; scale bar 100 µm. (*b*) Electron micrograph of an individual potato protease inhibitor crystal; scale bar 1 µm. (*c*) Electron diffraction of a negatively stained potato protease inhibitor crystal.

investigate further strands as we wanted to limit the number of initial variables for the selected heterogeneous substrate.

Our studies on heterogeneous crystallization were extended further to other proteins that are more difficult to crystallize. Of special interest to us was the potato protease inhibitor 6.1, as this protein is not easy to crystallize and its structure has still not been resolved by X-ray crystallography (Thomassen *et al.*, 2004). The crystals are difficult to manipulate and all attempts to soak them with heavy metals in order to obtain phase information have so far been unsuccessful. Moreover, crystals tend to intergrow, making the formation of large single crystals suitable for X-ray diffraction rather difficult. Potato protease inhibitor was observed to crystallize heterogeneously readily on the hair fibres, as shown in Fig. 2(*a*). Moreover, we could easily select individual crystals and image them (Fig. 2*b*), showing that the crystals are suitable for electron crystallography studies (Fig. 2*c*). Needle-like crystals on the hair surface were also obtained with glucose isomerase and Fab fragment 54. In the case of glucose isomerase, we also observed bulk crystals that usually appeared at the extremities of the fibres. In the presence of hair strands, glucose isomerase was crystallized at a twofold lower protein concentration (15 mg ml^{-1}) than necessary for homogeneous crystallization of the protein in bulk solution. When hair fibres were introduced into crystallization droplets of the Fab fragment and potato protease inhibitor, the protein was observed to nucleate preferentially on the surface of the hair in both cases. In the case of the Fab fragment, crystals appeared in bulk solution as well. Potato protease inhibitor crystals were also obtained in droplets to which protein precipitate was added.

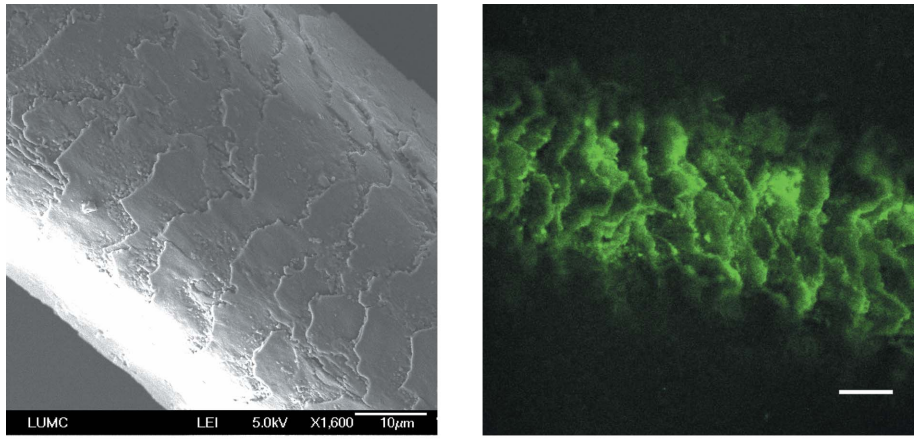

(*a*) (*b*)

Figure 3
Visualization of protein distribution by confocal fluorescent microscopy on the surface of human hair fibres. (*a*) Scanning electron micrograph of a human hair fibre, showing regularly repeated terraces on the surface. Scale bar 10 µm. (*b*) Distribution of protein on the surface of a hair fibre in crystallization droplets containing 1.6 *M* sodium chloride and 0.1 *M* sodium acetate pH 4.5 at a protein concentration of 0.5 mg ml^{-1} fluorescently labelled lysozyme. The green signal on the confocal photograph indicates the presence of fluorescent protein. The stronger the signal is, the more fluorescent protein is accumulated. The dark parts of the photo indicate the absence of fluorescent protein. Scale bar, 20 µm.

3.2. The mechanism of heterogeneous nucleation

Our experiments show that the surface of a hair is an effective nucleant for proteins. In order to understand this, we further investigated the effects of various chemical and morphological properties of the hair surface.

Keratins are the most predominant proteins in hair. They are ordered and may provide a semicrystalline interface at the surface. Their pI varies from 4.7 to 8.5, which provides some buffering properties to the system. Moreover, the surface of the hair is structured: regularly repeating overlapping terraces of different size and depth can be recognized in scanning electron micrographs, as shown in Fig. 3(*a*). In order to understand the mechanism of the observed heterogeneous crystallization, all the previously discussed properties needed to be excluded one by one. For this purpose, the fibres were treated with various chemicals: petroleum ether, ethanol and sodium hydroxide. After washing with mother liquor, they were introduced into crystallization droplets. Petroleum ether is well known as a delipidifying agent and is used routinely in phytochemistry. Ethanol is not only delipidifying but is also a moderate denaturing agent for proteins. Sodium hydroxide is a severe denaturing agent for proteins at the concentration used. After 24 h no crystallization was observed on fibres treated with sodium hydroxide. Only 'sea-urchin' crystals were noticed on the hair treated with ethanol, while both macro and 'sea-urchin' crystals were found on fibres treated with petroleum ether. All experiments were performed three times and the same results were obtained. This suggested that the removal of the lipids from the hair surface does not essentially influence the crystallization behaviour. Full loss of nucleation, inferred from the absence of crystals, was observed when the surface keratins were denatured and most probably the terraced structures were also etched away by sodium hydroxide. However, based on this experiment we could not distinguish between the importance of the chemical role of the surface proteins and the structure that they form: the effect of the surface structure and the role of the overlapping terraces, if any, remained unclear. We made a polymer replica of a hair, including its terraced surface, and set up a series of crystallization trials. Protein crystals were observed to grow occasionally on the polymer substrates, but there was no clear preference, contrary to the crystallization droplets with natural hair fibres. We concluded that the presence of keratin seems to be essential for nucleation.

To visualize the distribution of lysozyme on the hair surface, fluorescence studies were performed with labelled protein. In order to distinguish between the proteins of the hair fibres, which fluoresce mostly in the red, and the lysozyme (nonfluorescent in the visible spectrum), the latter was labelled with green fluorescing dye. We verified that this

modification did not influence crystallization (data not shown). At a protein concentration of 7.5 mg ml^{-1} labelled protein, heterogeneous crystallization could be followed, but the overall fluorescent signal was too strong to differentiate concentration differences next to or on the fibres. However, at a concentration of 2.5 mg ml^{-1} we observed a non-uniform distribution of lysozyme on the hair surface. At 1.0 and 0.5 mg ml^{-1} protein concentration we could clearly visualize that there is a much higher protein accumulation on the edges of the terraces (Fig. 3*b*). When fibres were pre-incubated overnight with 1 mg ml^{-1} nonfluorescent lysozyme under crystallization conditions (0.1 *M* acetate buffer pH 4.5, 1.6 *M* NaCl) and 0.5 mg ml^{-1} labelled protein was then added, a green signal was detected at the edges of the cuticles, suggesting that the protein binding is reversible in view of the apparent exchange of fluorescent *versus* nonfluorescent protein.

In dynamic AFM studies we followed the initial protein aggregation and crystal formation on the hair surface at a higher resolution. Imaging on the sharp edges was not possible as the height differences caused retraction of the AFM tip. In most of the cases, protein aggregates were observed to form on rougher parts or 'irregularities' of the scanned areas, such as clumps or scratches on the flat hair surface. When scanning was performed on relatively flat parts of the hair cuticles, no aggregation was observed during at least a few hours of imaging. However, we also observed that the scanning tip interfered with crystallogenesis, possibly by disturbing pre-nuclei.

3.3. Cryo-electron microscopy and crystallographic studies on small three-dimensional protein crystals

Small protein crystals are generally considered to not be suitable for crystallographic studies. Whereas this assumption is valid for X-ray single crystal diffraction, it is not true for electron diffraction. Our studies show that using cryo-electron microscopy, good diffraction information can be obtained from crystals with sizes in the range 50–300 nm. In fact, for electron-diffraction experiments the crystals have to be very thin because the interaction of electrons with matter is much larger (10^6) than that with X-rays.

For our experiments we used nano-sized lysozyme and potato protease inhibitor crystals grown on strands of hair. The advantage of using heterogeneous crystallization in this case was that by manipulating only the surface itself, all the small crystals could be transferred easily onto an electron microscopy grid. No additional 'fishing' techniques were needed. Plunge-frozen lysozyme crystals (Fig. 1*d*) diffracted to a resolution of about 3.5 Å (Fig. 1*e*) and we are currently pursuing this line of research, aiming to improve the diffraction and to collect full three-dimensional data sets.

4. Conclusions

We identified human hair to be a versatile nucleant surface and applied it successfully to the crystallization of various proteins. Moreover, despite the rather complex mechanism of heterogeneous crystallization, we discovered that the surface properties and the chemical composition together define the nucleation properties of the selected surface. No significant change in crystallization behaviour was observed after modifying the natural hair fibres with petroleum ether, while destroying the keratin with ethanol or sodium hydroxide caused partial and full loss of nucleation properties, respectively. A polymer replica of a hair fibre introduced into a crystallization experiment did not possess the nucleant properties of the natural fibres. On the basis of these observations, we conclude that the native protein surface is vital for nucleation and that the lipid layer is not required. AFM imaging combined with confocal fluorescence studies of the surface of hair fibres in crystallization conditions indicated that the structured surface also plays an important role in the nucleation. Furthermore, we showed by confocal imaging that there is an uneven distribution of protein on the nucleant substrate in crystallization conditions, which may explain the strong nucleating activity of hair fibres.

It has been observed by us and others that protein crystals tend to appear on the edges of natural or engineered nucleant surfaces (McPherson & Shlichta, 1987; D'Arcy *et al.*, 2003). To date, this phenomenon has remained somewhat enigmatic. Here, we provide visual evidence for protein accumulation on the edges of such a nucleant substrate. According to the classical nucleation theory, fluctuations in protein concentration are the driving force for crystallization.

By using heterogeneous nucleants, the high kinetic barrier of spontaneous nucleation can be bypassed. However, most of the initial trials produce only nanocrystals or microcrystals that require further improvement in order to be used for X-ray studies. Optimization is difficult to automate since it must be adapted to each case individually. Here, we show that nano-sized crystals, provided they are well ordered, can be used for electron crystallography studies. Solving structures using electron diffraction data from three-dimensional protein crystals is not yet feasible, but if certain technical obstacles can be overcome it may provide an excellent alternative to X-ray diffraction for proteins that only produce very small crystals.

The authors would like to thank Gerda Lamers for help with confocal fluorescent microscopy, Henk Koerten and Roman Koning for help with electron-microscopy photographs, Allard Katan and Marteen van Es for assistance with atomic force microscopy experiments and Ellen Thomassen for the kind gift of protease serine inhibitor protein. This work was supported by a grant from FOM (Stichting voor Fundamenteel Onderzoek der Materie), The Netherlands.

References

Berne, J. B. & Pecora, R. (1976). *Dynamic Light Scattering*. New York: Wiley & Sons.

Bodenstaff, E. R., Hoedemaeker, F. J., Kuil, M. E., de Vrind, H. P. M. & Abrahams, J. P. (2002). *Acta Cryst.* D**58**, 1901–1906.

Cacciuto, A., Auer, S. & Frenkel, D. (2004). *Nature (London)*, **428**, 404–406.

Chayen, N. E., Saridakis, E., El Bahar, R. & Nemirvsky, Y. (2001). *J. Mol. Biol.* **312**, 591–595.
Dale, G. E., Oefner, C. & D'Arcy, A. (2003). *J. Struct. Biol.* **142**, 88–97.
D'Arcy, A., Mac Sweeney, A. & Haber, A. (2003). *Acta Cryst.* D**59**, 1343–1346.
Fermani, S., Falini, G., Minnucci, M. & Ripamonti, A. (2001). *J. Cryst. Growth*, **224**, 327–334.
George, A. & Wilson, W. (1994). *Acta Cryst.* D**50**, 361–365.
Hemming, S. A., Bochkarev, A., Darst, S. A., Kornberg, R. D., Ala, P., Yang, D. S. C. & Edwards, A. M. (1995). *J. Mol. Biol.* **246**, 308–316.
Lorber, B., Jenner, G. & Giegé, R. (1996). *J. Cryst. Growth*, **158**, 103–117.
McPherson, A. & Shlichta, P. J. (1987). *J. Cryst. Growth*, **85**, 206–214.
Narayanan, J. & Liu, X. Y. (2003). *J. Biophys.* **84**, 523–532.
Roon, A. M. M. van, Pannu, N. S., de Vrind, J. P. M., van der Marel, G. A., van Boom, J. H., Hokke, C. H. & Abrahams, J. P. (2004). *Structure*, **12**, 1227–1236.
Sanjoh, A., Tsukihara, T. & Gorti, S. (2001). *J. Cryst. Growth*, **232**, 618–628.
Schmauder, R., Schmidt, T., Abrahams, J. P. & Kuil, M. E. (2002). *Acta Cryst.* D**58**, 1536–1541.
Thomassen, E. A., Pouvreau, L., Gruppen, H. & Abrahams, J. P. (2004). *Acta Cryst.* D**60**, 1464–1466.
Velev, O. D., Kaler, E. W. & Lenhoff, A. M. (1998). *J. Biophys.* **75**, 2682–2697.